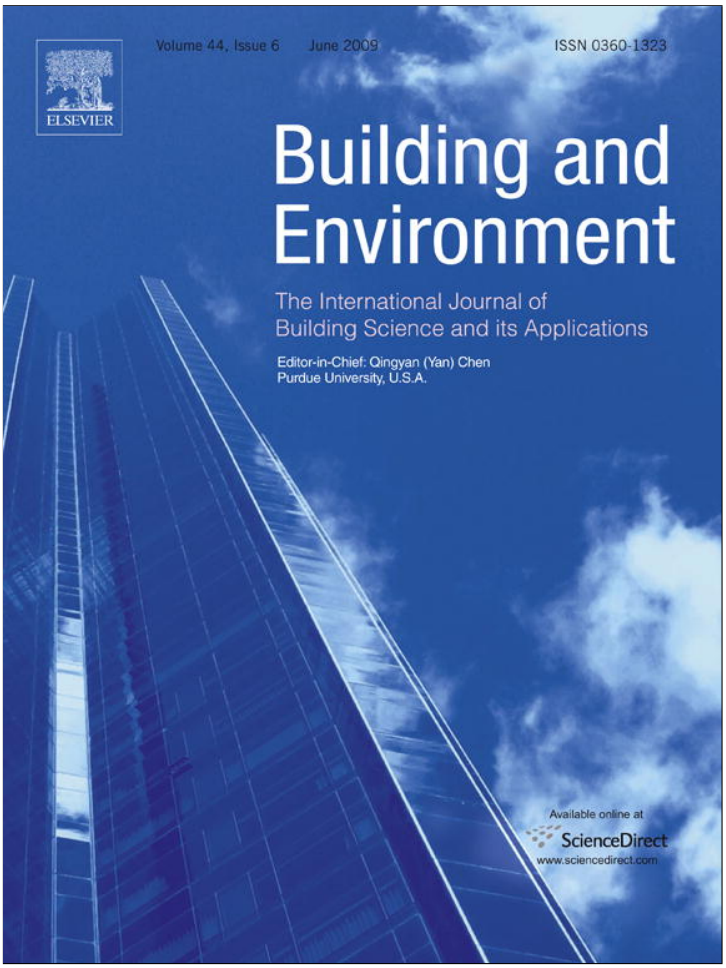

Building and Environment 44 (2009) 1318–1327

Contents lists available at ScienceDirect

Building and Environment

journal homepage: www.elsevier.com/locate/buildenv

Transient radon diffusion through radon-proof membranes: A new technique for more precise determination of the radon diffusion coefficient

Martin Jiranek, Zbynek Svoboda*

Department of Building Structures, Faculty of Civil Engineering, Czech Technical University, Thakurova 7, 166 29 Prague, Czech Republic

ARTICLE INFO

Article history:
Received 29 July 2008
Received in revised form
20 September 2008
Accepted 29 September 2008

Keywords:
Radon diffusion coefficient
Transient radon diffusion
Radon-proof membrane
Numerical analysis

ABSTRACT

The following paper is focused on the numerical modelling of the transient radon diffusion through radon-proof membranes during the measurement of their radon diffusion coefficient. The major aim of such numerical modelling is to increase the accuracy of radon diffusion coefficients derived from the measured data sets. The developed complex "transient" numerical model is able to calculate the radon diffusion coefficient with sufficient accuracy from almost any data set – even from a short-time measurement with a non-linear course of results. This numerical model can also be used for various analyses of transient radon transfer processes (e.g. for the calculation of radon distribution curves within the membrane). The following paper presents governing equations for the simulation model, together with a brief description of algorithms incorporated in the newly developed software package, which can be used either for the assessment of the radon diffusion coefficient from any data set or for the general analyses of unsteady radon transfer within the measuring device. Several transient model analyses are also presented together with an example of the determination of the radon diffusion coefficient from the measured data.

1. Introduction

The effectiveness of a radon-proof membrane is commonly expressed by means of its radon diffusion coefficient (sometimes also called radon permeability). Although there are several slightly different measuring methods for this quantity, they have the same principle. The sample of radon-proof membrane is placed between two gas-tight containers and the joint is carefully sealed (Fig. 1). The source container is connected to an efficient radon source, which is able to generate a very high radon concentration in the container for a shorter or longer time from the start of the measurement. Radon diffuses subsequently through the sample to the receiver container. The increase of radon concentration in the air is measured in the source container as well as in the receiver container.

The containers themselves are not measuring units in most existing devices. Radon concentration is commonly measured by scintillation detectors [1,2] or semiconductor detectors [3], which are connected to the containers (Fig. 1). The main drawbacks of this arrangement are as follows: (a) potential dependence of the measured values on the volume of each container and on the location of detectors and (b) the delayed response of the detectors because radon gets to them through the containers. A new technique [4] – which was also used during the preparation of this paper – removes the disadvantages mentioned above by identifying the containers with measuring units (Fig. 1). So both containers serve at the same time as ionisation chambers operating in current mode with a sensitive detection volume (volume of each container) of 2.02 l. A fully automatic measuring device enables continuous monitoring of radon concentration in both containers at one-minute intervals.

As soon as the measurement is finished, the radon diffusion coefficient can be derived by means of various procedures from the time-dependent courses of radon concentrations in both containers.

It can be seen that the whole measuring process consists of two separate parts: the first is the measurement of radon concentrations on both sides of the tested membrane and the second is the calculation of the radon diffusion coefficient using mathematical processing of the measured data. As the radon diffusion coefficient is a very small number (typically from 1×10^{-8} to 1×10^{-15} m^2/s), the accuracy of both steps is crucial.

2. Existing methods and their problems

Main problems of the first – measurement – phase are as follows: (a) the determination of the time, which is necessary for

* Corresponding author. Tel.: +420 224 355 402.
E-mail address: svobodaz@fsv.cvut.cz (Z. Svoboda).

0360-1323/$ – see front matter © 2008 Elsevier Ltd. All rights reserved.
doi:10.1016/j.buildenv.2008.09.017

Nomenclature

A	area of the sample taken from a radon-proof membrane [m^2]
C	radon concentration [Bq/m^3]
C_a	radon concentration in a particular container of the measuring device [Bq/m^3]
C_n	vector of radon concentrations in nodes of the finite element mesh [Bq/m^3]
C_{rc}	radon concentration in the receiver container of the measuring device [Bq/m^3]
C_s	radon concentration on the surface of the sample [Bq/m^3]
C_{sc}	radon concentration in the source container of the measuring device [Bq/m^3]
C_{ssc}	radon concentration on the surface of the sample exposed to the source container [Bq/m^3]
C_{src}	radon concentration on the surface of the sample exposed to the receiver container [Bq/m^3]
d	thickness of the sample [m]
d_e	length of one-dimensional finite element [m]
D	radon diffusion coefficient [m^2/s]
E	radon exhalation rate from the sample to the receiver container [$Bq/(m^2\,s)$]
h	radon transfer coefficient [m/s]
K_c	capacity matrix
K_d	conductance matrix
K_h	boundary conditions matrix
$K_{h,s}$	boundary conditions matrix of the finite element exposed to the source container
$K_{h,r}$	boundary conditions matrix of the finite element exposed to the receiver container
K_λ	radioactive decay matrix
l	radon diffusion length [m]
n	air change rate in the receiver container of the measuring device [1/s]
N	vector of interpolation functions
P	radon transmittance [m/s]
q_h	boundary conditions vector
$q_{h,s}$	boundary conditions vector of the finite element exposed to the source container
$q_{h,r}$	boundary conditions vector of the finite element exposed to the receiver container
t	time [s]
V	volume of the receiver container of the measuring device [m^3]
x	distance from the surface of the radon-proof membrane [m]
Δt	time difference between time steps (i) and ($i-1$) [s]
λ	radon decay constant [2.1×10^{-6} 1/s]
$\partial/\partial n$	derivative in the direction of external normal to the boundary

the establishment of a steady-state radon diffusion through the sample; and (b) the determination of the minimum radon concentration in the source container, which is needed for the development of sufficiently high (i.e. well detectable) radon concentration in the receiver container. In the second – calculation – step of the measuring procedure, the usual source of errors can be found in the universal use of simple numerical techniques, although they are valid (and accurate enough) only for certain materials and/or in certain conditions.

The assumption of linear radon distribution within the measured sample belongs among such typical conditions (although it is completely inappropriate for the radon-proof barriers, due to their specific properties, as was already clarified in Ref. [5]). Nevertheless, with this supposition, the radon diffusion coefficient can be derived from its frequently used definition (cited also in Ref. [5]):

$$D = d\frac{E}{C_{ssc} - C_{src}} \tag{1}$$

with surface radon concentrations taken in a simplified way as relevant radon concentrations in the source and receiver containers:

$$C_{ssc} = C_{sc}(t_2) \text{ and } C_{src} = C_{rc}(t_2) \tag{2}$$

and the radon exhalation rate derived usually from the equation

$$C_{rc}(t_2) = C_{rc}(t_1)e^{-\lambda(t_2-t_1)} + \frac{EA}{V\lambda}\left[1 - e^{-\lambda(t_2-t_1)}\right] \tag{3}$$

as

$$E = \frac{\lambda V\left[C_{rc}(t_2) - C_{rc}(t_1)\,e^{-\lambda(t_2-t_1)}\right]}{A\left[1 - e^{-\lambda(t_2-t_1)}\right]}. \tag{4}$$

Eq. (3) defines the radon concentration in the receiver container at time t_2 as a function of the radon concentration in the previous time step and the increase of radon concentration caused by the radon exhalation rate from the sample. Both the former radon concentration $C_{rc}(t_1)$ and the increase of radon concentration (EA)/

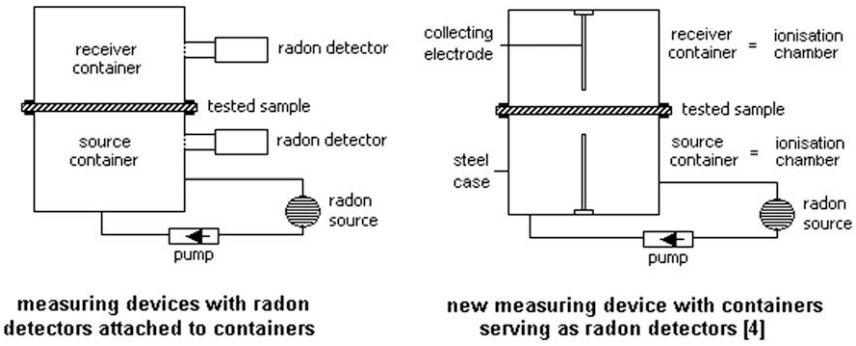

Fig. 1. Scheme of measuring devices used for the determination of the radon diffusion coefficient.

($V\lambda$) are multiplied by exponential terms which express the effects of the radon decay process (in a usual form of an exponential decay equation).

A more sophisticated technique [3] uses the assumption of linear increase of radon concentrations in both containers of the measuring device. The radon diffusion coefficient is subsequently calculated from

$$D = dP \tag{5}$$

with the radon transmittance P obtained by means of an iterative process from

$$\frac{1}{b-1-\frac{\lambda V}{PA}}\ln\left[\frac{a+\left(b-1-\frac{\lambda V}{PA}\right)C_{\mathrm{rc}}(t_1)}{a+\left(b-1-\frac{\lambda V}{PA}\right)C_{\mathrm{rc}}(t_2)}\right] = \frac{PA}{V}(t_1-t_2) \tag{6}$$

and quantities a and b derived from the reciprocal dependence of radon concentrations in both containers (based on measured data):

$$C_{\mathrm{sc}} = a + bC_{\mathrm{rc}}. \tag{7}$$

Iteration is also needed for the determination of the radon diffusion coefficient in another calculation method [6], which assumes that the steady state is established at the end of the measurement and the radon diffusion coefficient can be derived from

$$D = \lambda l^2. \tag{8}$$

The radon diffusion length l is calculated iteratively from

$$\frac{E}{C_{\mathrm{sc}}} = \frac{2\lambda l}{\left(\mathrm{e}^{d/l}-\mathrm{e}^{-d/l}\right)} \tag{9}$$

supposing that the radon concentration in the source container C_{sc} is constant and the radon exhalation rate E can be derived from Eq. (4). The air change rate in the receiver container is expected to be negligible in this method as well as in the methods described earlier.

Three examples of simple calculation procedures clearly show that their results can be accurate only when all the assumptions are fulfilled. That can be quite difficult especially in the case of low permeable membranes and/or low radon concentration in the source container. The measurement can be – and often is – stopped prematurely and the consequent use of simple calculation techniques can lead to a considerable loss of accuracy of the calculated radon diffusion coefficient. Another problem originates in the fact that often-expected linear radon distribution within the measured membrane is rather rare – as will be shown later on.

All the problems mentioned above make the creation of a universal numerical model of the measuring procedure highly important. Such a model could be used for deep analyses of the transient radon diffusion through the measured sample from the start to the end of the measurement. It would also help the user to test various, more complex measurement strategies (e.g. the two-stage measurement with full ventilation of the receiver container between both stages). The discussed numerical model could also be used for the assessment of the necessary measurement time and the necessary output of the radon source. And last but not least, the calculation of the radon diffusion coefficient based on this numerical model would be considerably more universal and precise because it would use the input data describing the whole time-dependent measuring process and not only the final hypothetical "steady state" or a chosen part with linear changes in radon concentrations in both containers. The following chapter is focused on governing equations, which can be used for such a numerical model.

3. Procedures and governing equations

3.1. Modelling of transient radon diffusion through radon-proof barriers

The governing equation, which describes radon distribution in radon-proof barriers, is a standard one-dimensional partial differential equation

$$\frac{\partial}{\partial x}\left(D\frac{\partial C}{\partial x}\right) - \lambda C = \frac{\partial C}{\partial t}, \tag{10}$$

where x ranges from 0 (the lower surface of the barrier) to d (the upper surface of the barrier). As Eq. (10) is used in this paper to analyse transient radon diffusion through the radon-proof barrier during the measurement of its radon diffusion coefficient, the origin of time t in Eq. (10) is set to the beginning of the measurement. At that time, $t_0 = 0$ s, the initial condition within the whole x-range is taken as

$$C = C_0 = 0. \tag{11}$$

The initial radon concentration in the radon-proof barrier is taken as 0 Bq/m^3 because it is assumed that the sample of the barrier is only fixed to the measuring device at that moment. The boundary condition for Eq. (10) can be expressed on both sides of the radon-proof barrier (i.e. for $x = 0$ as well as for $x = d$) as

$$-D\frac{\partial C}{\partial x} = h(C_{\mathrm{s}} - C_{\mathrm{a}}). \tag{12}$$

Consequently, the value of C_{a} can be either the known radon concentration in the source container:

$$C_{\mathrm{a}} = C_{\mathrm{sc}}, \tag{13}$$

(applicable for $x = 0$) or the initially unknown radon concentration in the receiver container (applicable for $x = d$). This value must be calculated for the time step (i) from the previous step ($i-1$) using the equation

$$C_{\mathrm{a}} = C_{\mathrm{rc},i} = C_{\mathrm{rc},i-1}\,\mathrm{e}^{-(\lambda+n)\Delta t} + \frac{E_{i-1}A}{V(\lambda+n)}\left(1-\mathrm{e}^{-(\lambda+n)\Delta t}\right), \tag{14}$$

which is derived from Eq. (3) and includes in addition the effect of the ventilation of the receiver container (expressed by means of its air change rate n). This effect can be important especially in the cases with significant leaks in the sealing between the sample and the receiver container because the ventilation of the receiver container leads to an enlarged decrease of radon concentration.

The radon exhalation rate from the radon-proof barrier to the receiver container in the time step ($i-1$) can be calculated from

$$E_{i-1} = h\left(C_{\mathrm{src},i-1} - C_{\mathrm{rc},i-1}\right) \tag{15}$$

with $C_{\mathrm{rc},0}$ taken as a known initial value (usually close to 0 Bq/m^3) and the radon transfer coefficient h derived using the procedure described in Ref. [7].

The numerical solution of Eq. (10) with conditions (11) and (12) can be obtained by means of the finite element method (FEM) using the standard Galerkin approach. This approach belongs among weighted residuals methods and thus the derivation of the finite element formulation starts with the equation

$$\int_0^{d_{\mathrm{e}}}\left[\frac{\partial}{\partial x}\left(D\frac{\partial C}{\partial x}\right) - \lambda C - \frac{\partial C}{\partial t}\right]N\mathrm{d}x = 0, \tag{16}$$

which is a mathematical expression of the requirement that the residual of the numerical solution of Eq. (10) must be orthogonal to

the interpolation functions N [8]. The unknown function C in Eq. (16) is taken as an approximation

$$C = N^T C_n, \tag{17}$$

where C_n is a vector of unknown radon concentrations in the nodes of the created FEM mesh and N is a vector of known interpolation functions, which are dependent on the types of chosen finite elements. In this case, it is possible to use the simplest one-dimensional finite elements with two nodes and linear approximation (they correspond to the partial fractions of the thickness of the radon-proof barrier). Two interpolation functions are used for each finite element:

$$N_1 = 1 - \frac{x}{d_e} \text{ and } N_2 = \frac{x}{d_e} \tag{18}$$

with x ranging from 0 (node 1) to d_e (node 2).

The general finite element formulation can be finally derived using three steps: (a) substitution of Eq. (17) into Eq. (16); (b) integration by parts applied to the first term in Eq. (16) and (c) introduction of the boundary condition (12) into modified Eq. (16). As a result, the FEM formulation can be written in the form

$$(K_d + K_\lambda + K_h)C_n + K_c\frac{dC_n}{dt} = q_h, \tag{19}$$

where the conductance matrix K_d is defined as

$$K_d = \int_0^{d_e} D\left(\frac{dN}{dx}\frac{dN^T}{dx}\right)dx = \frac{D}{d_e}\begin{bmatrix} 1 & -1 \\ -1 & 1 \end{bmatrix}, \tag{20}$$

the radioactive decay matrix K_λ as

$$K_\lambda = \int_0^{d_e} \lambda NN^T dx = \frac{\lambda d_e}{6}\begin{bmatrix} 2 & 1 \\ 1 & 2 \end{bmatrix}, \tag{21}$$

and the capacity matrix K_c as

$$K_c = \int_0^{d_e} NN^T dx = \frac{d_e}{6}\begin{bmatrix} 2 & 1 \\ 1 & 2 \end{bmatrix}. \tag{22}$$

The final formulations of the matrices presented in Eqs. (20–22) were derived using the interpolation functions defined in Eq. (18).

The boundary related matrix K_h and vector q_h in Eq. (19) are non-zero for two finite elements only. The first one is located on the lower side of the radon-proof barrier, which means that it is exposed to the source container and its matrix K_h and vector q_h are therefore

$$K_{h,s} = \begin{bmatrix} h & 0 \\ 0 & 0 \end{bmatrix} \text{ and } q_{h,s} = \begin{Bmatrix} hC_{sc} \\ 0 \end{Bmatrix} \tag{23}$$

with radon concentration C_{sc} defined in Eq. (13). The second finite element, with non-zero boundary matrix and vector, is located on the opposite side of the radon-proof barrier. Consequently, its matrix K_h and vector q_h have different definitions:

$$K_{h,r} = \begin{bmatrix} 0 & 0 \\ 0 & h \end{bmatrix} \text{ and } q_{h,r} = \begin{Bmatrix} 0 \\ hC_{rc} \end{Bmatrix}, \tag{24}$$

where radon concentration C_{rc} is calculated for each time step from Eq. (14).

The general FEM formulation (19) is valid for each finite element as well as for the entire analysed region (i.e. in this case for the radon-proof barrier). Relevant matrices and vectors for the entire region are created by localisation of the individual element matrices and vectors. More details about this process can be found, for example, in Ref. [8].

The last problem of the numerical solution of Eq. (19) is the time-dependency of the boundary vector q_h and the vector of unknown nodal values C_n. To handle this difficulty, it is assumed that both vectors can be expressed in the time interval from $(i-1)$ to (i) as

$$C_n = \varepsilon C_{n,i} + (1-\varepsilon)C_{n,i-1}, \tag{25}$$

$$q_h = \varepsilon q_{h,i} + (1-\varepsilon)q_{h,i-1}, \tag{26}$$

where ε is chosen as $0.5 \le \varepsilon \le 1$ in order to ensure the numerical stability of the calculation [8]. The usual recommended value is $\varepsilon = 0.5$, which was also used in the presented numerical solution of Eq. (10). Substitution of Eqs. (25) and (26) into Eq. (19) leads finally to a system of linear algebraic equations for unknown nodal values $C_{n,i}$:

$$\begin{aligned}\left[(K_d + K_\lambda + K_h)\varepsilon + \frac{K_c}{\Delta t}\right]C_{n,i} = {} & q_{h,i}\varepsilon + q_{h,i-1}(1-\varepsilon) + \\ & + \left[\frac{K_c}{\Delta t} - (K_d + K_\lambda + K_h)(1-\varepsilon)\right]C_{n,i-1}\end{aligned} \tag{27}$$

where initial radon concentrations $C_{n,0}$ are taken as radon concentrations C_0 from Eq. (11). The complete calculation process for time step (i) starts with the determination of boundary conditions, particularly with the calculation of the radon concentration in the receiver container $C_{rc,i}$ using Eq. (14). The boundary vectors $q_{h,i}$ for both boundary finite elements are subsequently calculated from Eqs. (23) and (24). The right hand side of Eq. (27) is then entirely known and the solution of Eq. (27) can be found using standard Gauss elimination. Known values from the previous time step $(i-1)$ are used throughout this process.

The developed TransRn software [9] calculates the FEM solution of radon concentrations in the radon-proof barrier in the regular mesh consisting of 50 one-dimensional finite elements. The usual width of an element is very small – ranging from 0.02 to 0.10 mm. The basic time step is taken as 360 s and the whole calculation time is derived from the condition that the radon concentration in the receiver container must reach a steady state. The calculation program also offers the option of modelling the two-stage measurement technique in which the receiver container is fully ventilated at the end of the first stage (i.e. at the moment when the radon concentration in the receiver container is steady and the measured barrier is saturated with radon). The boundary conditions for the second stage can be defined in a different way from the first stage and so it is possible to simulate various strategies for the measurement.

The TransRn software was created using Microsoft Visual Basic 6.0 as a typical Microsoft Windows application. The user can create, save, read and edit the input data files (in internal format) as well as the calculation protocols (in RTF format) and graphical outputs (in BMP format). The main window of the program with text and numerical input boxes is shown on Fig. 2.

3.2. Calculation of the radon diffusion coefficient

The numerical assessment of the radon diffusion coefficient by means of the IterRn software [9] uses as the basic input the measured, time-dependent values of radon concentrations in the source and the receiver containers. The calculation is based on the iterative numerical solution of Eq. (10). At the beginning of the procedure, the user sets the estimated range of the radon diffusion coefficient (lower limit, upper limit) and the step for the iteration (usually from 1/10 to 1/20 of the range). Subsequently, the transient radon diffusion through the radon-proof barrier is solved according to the method described above – in this first step, the radon

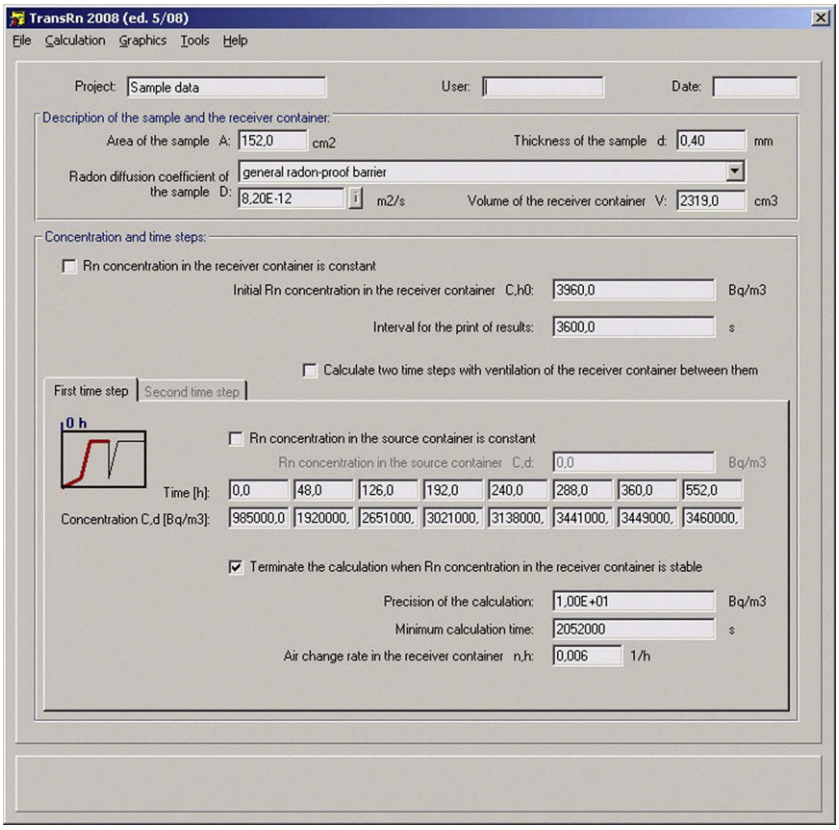

Fig. 2. Main window of TransRn software.

diffusion coefficient is taken as the chosen lower limit. The calculated time-dependent results of radon concentration in the receiver container are afterwards compared with the relevant measured data and the differences between both data sets are recorded. In the following steps, the whole procedure is repeated with continuously growing radon diffusion coefficient until its upper limit is reached. The final radon diffusion coefficient is the value for which the variations between calculated and measured data, such as the average difference or the sum of deviations, are minimal. The entire iteration process usually takes no more than 30 min on a typical contemporary PC.

The IterRn software was developed for the Microsoft Windows environment in the same way as the TransRn software. It uses standard MS Windows procedures and dialogs for creating, saving, reading and editing of the data files. The input values (i.e. the results of the measurement described above) can be either entered one by one into the input boxes on the program's main window or read directly from the record of the measurement (simple text file with values separated by commas).

4. Model analyses

Understanding of the complex radon transfer processes within both the measuring device and the measured sample of radon-proof barrier is essential for a measurement with a high level of accuracy. The fundamental correlations, e.g. between the radon distribution and the thickness of the sample or its radon diffusion coefficient, can be studied by means of the numerical modelling tools such as TransRn. The following results of several model analyses show some significant dependencies and general relations between the physical quantities involved in the radon transfer process.

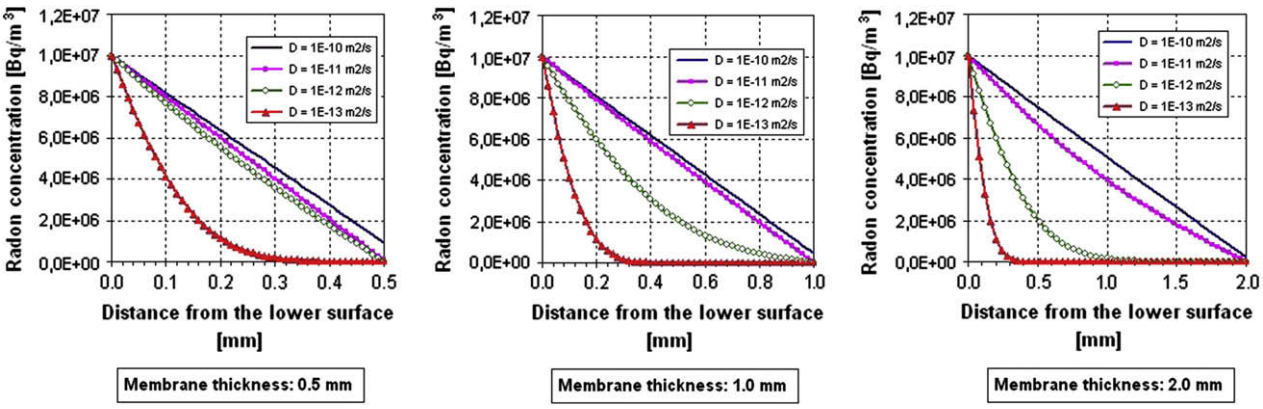

Fig. 3. Radon distribution within typical membranes shortly after the start of the measurement.

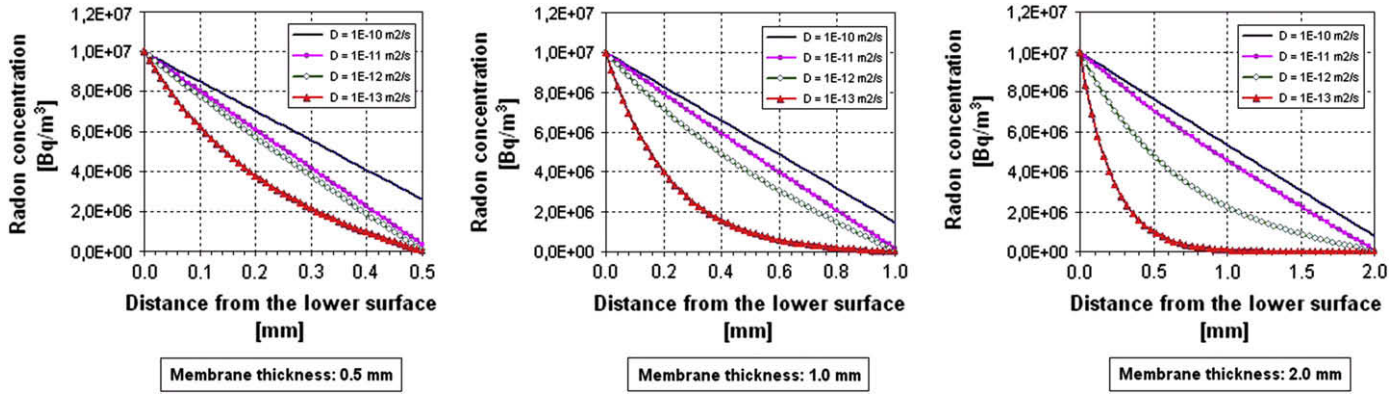

Fig. 4. Radon distribution within typical membranes at the end of the measurement.

4.1. Radon distribution within the radon-proof membrane

The radon concentration profile within the measured radon-proof membrane has in general the shape of an exponential function. In some cases, e.g. for very thin membranes with relatively high radon diffusion coefficient, the radon distribution can be almost linear. Nevertheless, this is not a typical situation because such highly radon-permeable membranes cannot usually be used as efficient radon-proof barriers.

Typical initial radon distributions within membranes with various thicknesses and various radon diffusion coefficients are presented on Fig. 3. This figure shows the calculated curves of radon concentration in the first characteristic moment: 24 h after the beginning of the measurement (i.e. after the moment when the radon concentration in the source container of the measuring device was set to a constant value of 10 MBq/m^3). It is obvious that radon penetrates in membranes with a low radon diffusion coefficient only to a depth of around 0.2 mm at this early measurement phase (see the curve for the radon diffusion coefficient $D = 1 \times 10^{-13}$ m^2/s). On the other hand, the radon distribution for the membranes with radon diffusion coefficients higher or equal to 1×10^{-11} m^2/s is almost linear from the very start of the measurement.

However, even for such highly permeable barriers, the final steady-state radon distribution (Fig. 4) differs from the initial state. The main reasons are as follows: (a) the measured sample is fully saturated with radon at the end of the measurement and (b) simultaneously the radon concentration in the receiver container is considerably higher than it was at the beginning. For various membranes, it takes various amounts of time to reach the final phase of the measurement (usually from 3 to 30 days). In this phase, the radon diffusion through the sample is not time-dependent and the final radon distribution within the sample is stable. All the radon concentration curves on Fig. 4 resemble the curves on Fig. 3 but they are shifted slightly higher on the right hand side and also in the centre part of the measured membrane.

The transient changes in radon concentration within the sample are also essential for the understanding of time-dependent radon diffusion processes. The radon distribution within a membrane with high radon permeability is practically linear at all registered time steps during the 12 days after the beginning of the measurement (Fig. 5). The same time-dependent curves for a high-quality radon-proof barrier create a noticeably different picture with clearly recognizable exponential lines (Fig. 6).

All the figures presented in this chapter are valid for the same measurement conditions. The initial radon concentration in the

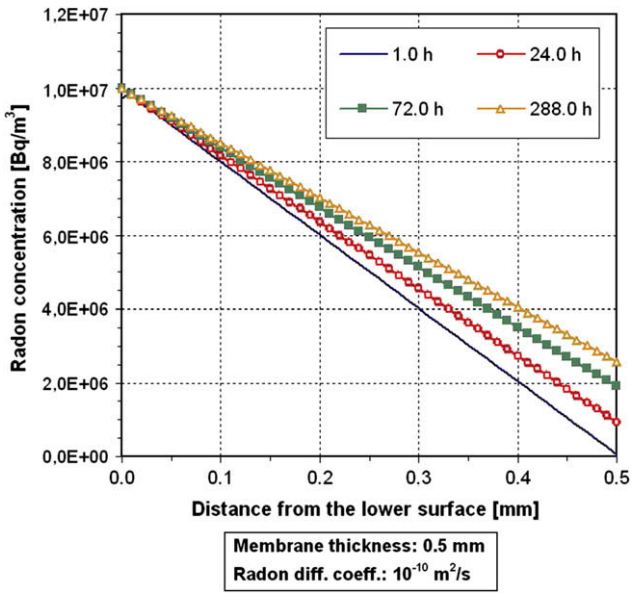

Fig. 5. Transient radon distribution within a thin membrane with high radon diffusion coefficient.

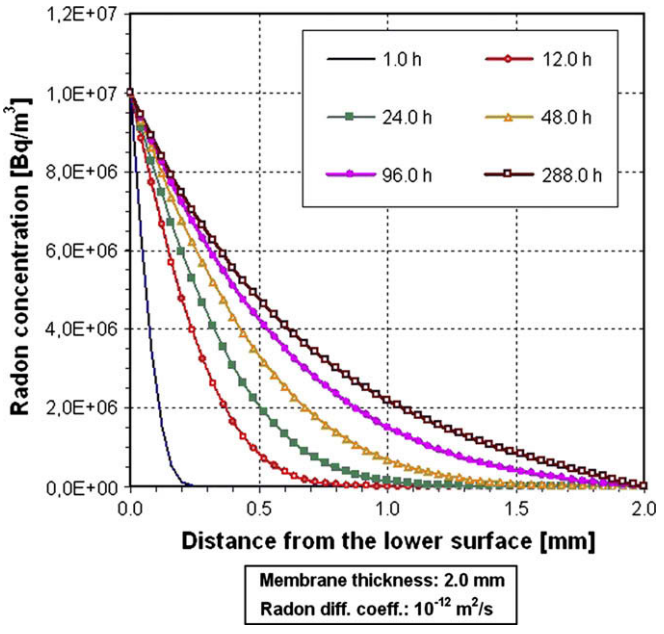

Fig. 6. Transient radon distribution within a high-quality radon-proof membrane.

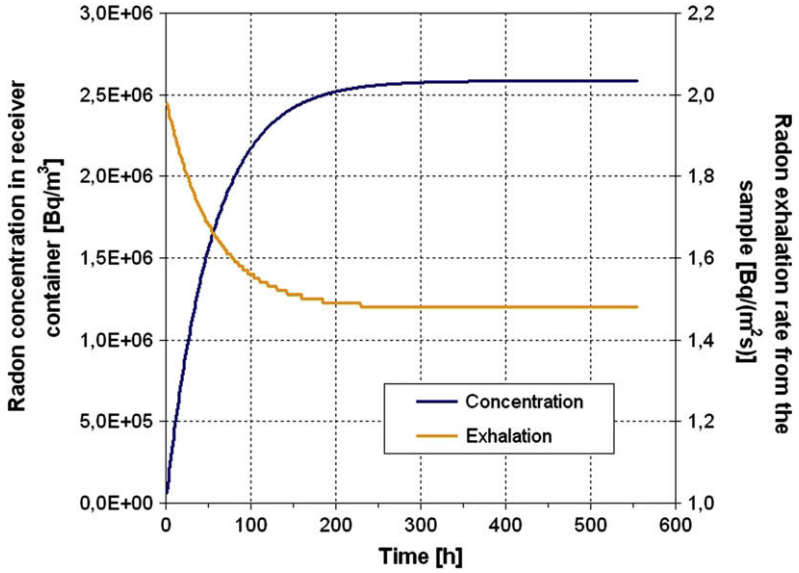

Fig. 7. Radon exhalation rate and radon concentration in the receiver container for a membrane with high radon permeability (thickness 0.5 mm, radon diffusion coefficient 1×10^{-10} m^2/s).

sample was 0 Bq/m^3, the radon concentration in the source container was taken as a constant value of 10 MBq/m^3 and the radon concentration in the receiver container was calculated from Eq. (14) assuming that the initial radon concentration in the receiver container was 50 Bq/m^3.

4.2. Radon concentration in the receiver container

Properties of the radon-proof membrane have a naturally strong impact on both the radon exhalation rate from the measured sample and the transient changes of the radon concentration in the receiver container of the measuring device.

Membranes with a high radon diffusion coefficient are well radon-permeable and therefore the maximum radon exhalation rate from the sample to the receiver container can be found at the beginning of the measurement (when there is the highest difference between the radon concentration on the upper surface of the sample and the radon concentration in the upper, receiver container). During the measurement, the radon concentration in the receiver container increases and subsequently the exhalation rate gradually decreases until a steady state is reached (Fig. 7).

The numerical modelling of the measurement of membranes with a low radon diffusion coefficient (1×10^{-11} m^2/s and lower) shows quite different results. Such membranes are excellent radon-proof barriers and therefore it usually takes a longer time to reach the steady state (Fig. 8). The radon exhalation rate is the highest at this final stage as well as the radon concentration in the receiver container. This is caused by extremely slow radon diffusion through the sample (see Fig. 6) due to which the radon concentration on its upper surface is close to the initial radon concentration in the upper, receiver container for a significantly long period. This is also the reason for the initial shape of both curves on Fig. 8. The length of this period depends on the thickness and on the radon diffusion coefficient of the sample. Membranes with lower radon permeability have these initial periods longer as it is more time-consuming to get them saturated with radon. The initial period can

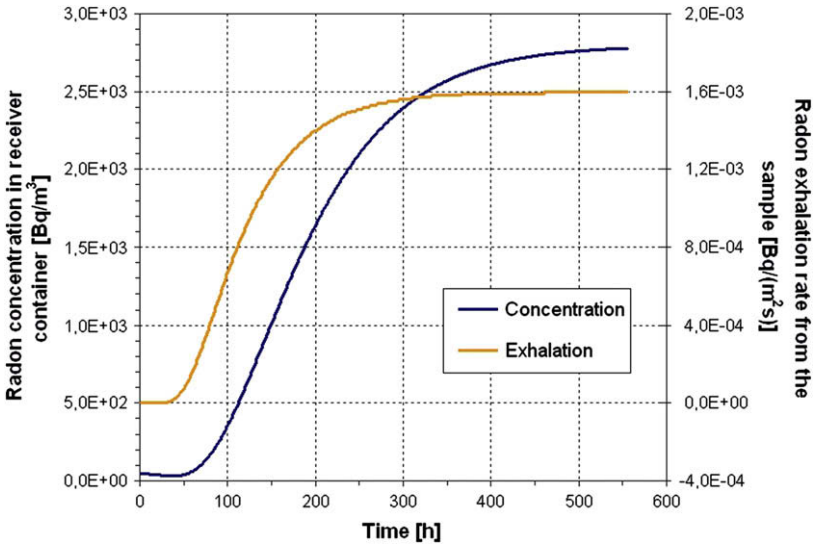

Fig. 8. Radon exhalation rate and radon concentration in the receiver container for the membrane with low radon permeability (thickness 2.0 mm, radon diffusion coefficient 1×10^{-12} m^2/s).

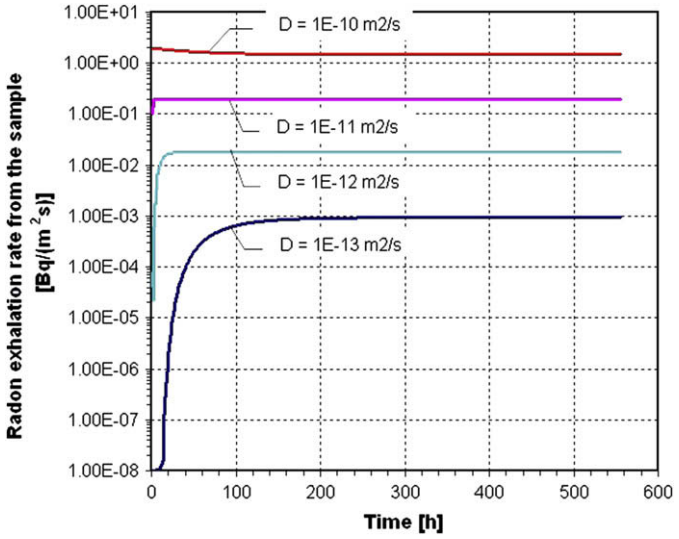

Fig. 9. Radon exhalation rates from 0.5 mm thick membrane exposed to the radon concentration of 10 MBq/m^3.

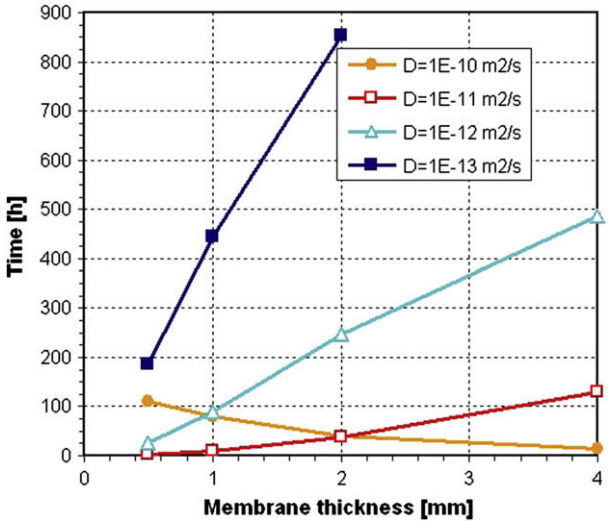

Fig. 11. Periods necessary for the establishment of the steady state (with changes in exhalation rates lower than 5%).

be generally observed within the first few days (up to 4 days) after the measurement has commenced. In this measuring phase, the commonly used linear approximation of the measured data, e.g. by means of Eqs. (5–7), can lead to serious errors in the evaluation of the radon diffusion coefficient.

Correlations between radon exhalation rates and the properties of the measured sample (radon diffusion coefficient and membrane thickness) are plotted as a function of time on Figs. 9, 10. These figures confirm that the exhalation rates from membranes exposed to the same radon concentration are proportional to their radon diffusion coefficients and inversely proportional to their thicknesses. Time intervals necessary for the establishment of the steady state can be also identified from these figures. It is seemingly surprising that the longest measurement times are required not only for thick membranes with low radon diffusion coefficient but also for very thin membranes with a radon diffusion coefficient of around 1×10^{-10} m^2/s. However, the explanation of this observation is very simple and can be understood from Fig. 7.

The minimum duration of the measurement from the start to the final steady state in dependence on the membrane thickness and its radon diffusion coefficient is summarized on Fig. 11. It can be seen that this period ranges from 3 to 30 days for typical radon-proof membranes with thicknesses from 0.5 to 4 mm and radon diffusion coefficients between 1×10^{-10} m^2/s and 1×10^{-13} m^2/s. Such long times are not convenient for practical measurements and so they are not usually respected. Unfortunately, this consequently leads to inaccuracies in the value of the radon diffusion coefficient derived from such non-steady data by means of simple equations such as Eqs. (8) and (9). More complex numerical modelling is the only way how to overcome this problem because it can help to determine the radon diffusion coefficient, even from the "transient" data sets for both containers of the measuring device (more details in the next chapter).

Numerical modelling can be also used for predictions of the minimal radon concentration in the source container for various types of measured membranes (in dependence on their thicknesses

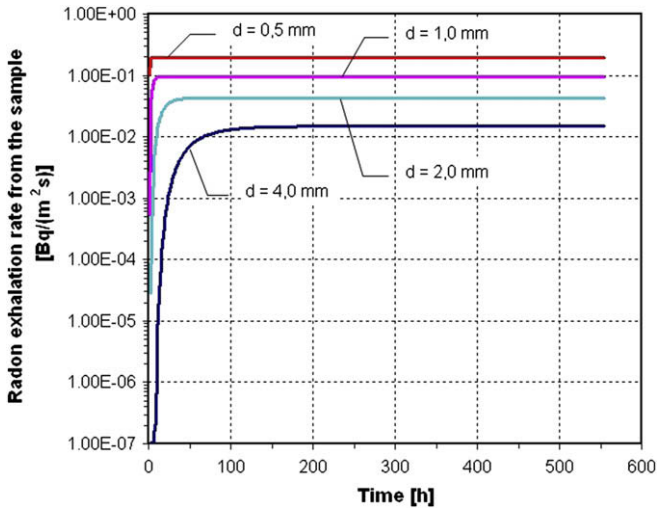

Fig. 10. Radon exhalation rates from a membrane with radon diffusion coefficient 1×10^{-11} m^2/s exposed to the radon concentration of 10 MBq/m^3.

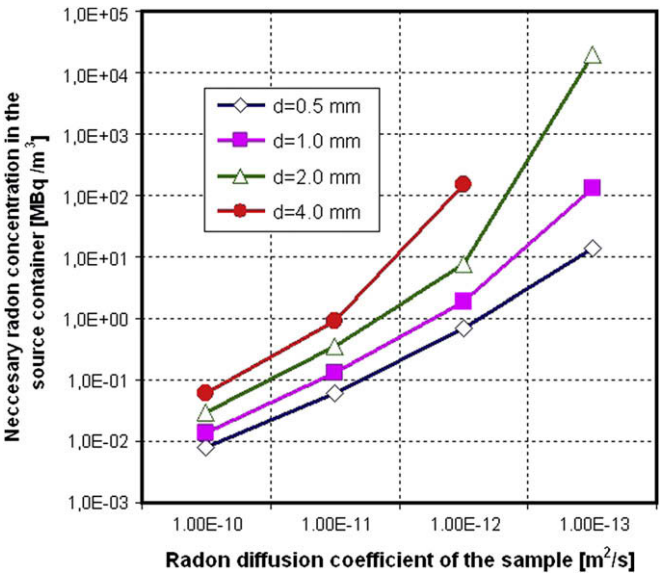

Fig. 12. Minimal radon concentration in the source container ensuring steady-state radon concentration of 2 kBq/m^3 in the receiver container.

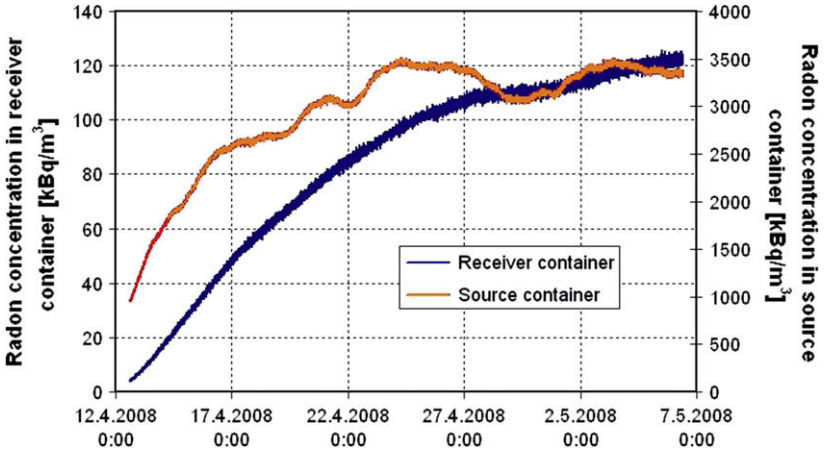

Fig. 13. Measured radon concentrations in the source and receiver containers.

and their estimated radon diffusion coefficients). Such predictions ensure that the radon concentration in the receiver container will be detectable by the applied measurement technique and the measurement uncertainties will be as low as possible. If we take, for instance, the typical value of 2 kBq/m^3 as a well detectable value of the radon concentration in the receiver container, the minimal radon concentrations in the source container can be predicted from Fig. 12. It can be seen that for this assumption, the radon concentration in the source container should be – for example – at least 1 MBq/m^3 for a membrane 0.5 mm thick if its estimated radon diffusion coefficient oscillates at around 1×10^{-12} m^2/s. The influence of the membrane thickness is highly important in this assessment: for the same estimated radon diffusion coefficient and 4 times higher thickness (2.0 mm), the source radon concentration must be at least 10 times higher (10 MBq/m^3).

5. Calculation of the radon diffusion coefficient from a measured data set

As was already mentioned, the numerical modelling of transient radon diffusion is a highly useful tool for the derivation of the radon diffusion coefficient. It is actually the only tool with sufficient accuracy in the cases when the measured radon concentrations in both containers are still unsteady and/or the radon distribution within the measured sample is exponential.

The whole assessment process – from the measured data to the numerical derivation of the radon diffusion coefficient by means of the IterRn software package [9] – is illustrated further on. The measured sample was taken from a 0.4 mm thick polyethylene radon-proof membrane. The area of the sample was 152 cm^2 and the volume of the receiver container was 2319 cm^3. The air change rate in the receiver container was expected to be almost negligible – only 0.006 1/h. The measured time-dependent radon concentrations in both containers of the measuring device are shown on Fig. 13. These detailed curves, which were obtained from the measurement with a time step of 2 min, were subsequently simplified into straight lines to make the input into the computer program possible (Fig. 14). The IterRn software calculated afterwards the radon diffusion coefficient using the iterative method described in Section 3.2. The value of the radon diffusion coefficient was determined as $D = 8.2 \times 10^{-12}$ m^2/s. The comparison between the measured radon concentration in the receiver container and the same quantity calculated for this radon diffusion coefficient is presented on Fig. 15.

It is interesting that the radon diffusion coefficient calculated via detailed numerical modelling is in this case higher than the same quantity derived by means of the simple calculation techniques

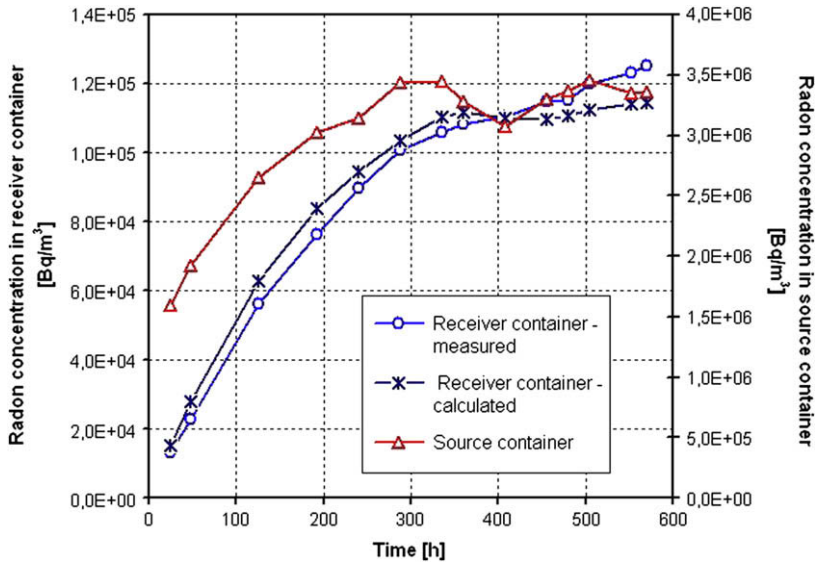

Fig. 14. Input data for the numerical modelling and its results.

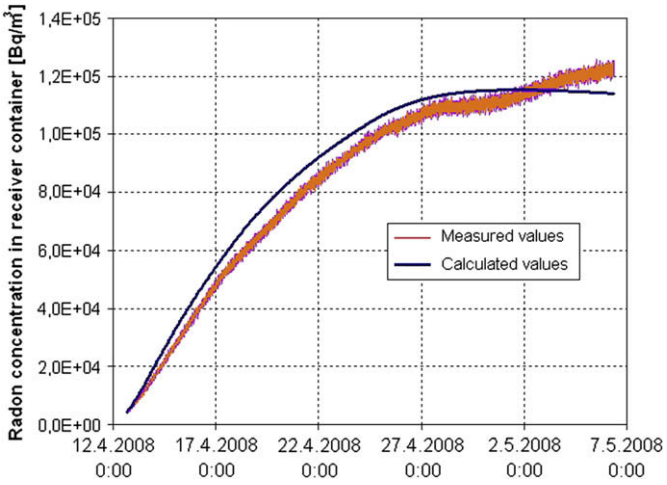

Fig. 15. Correlation between the measured and the calculated radon concentrations in the receiver container.

described in chapter 2. The differences are within a range from 15% to 33%, which is quite important considering the fact that a higher radon diffusion coefficient means higher radon permeability. Thus, the simple techniques in this case slightly overestimate the quality of the radon-proof membrane.

6. Conclusion

The developed computer programs IterRn and TransRn, which are based on the numerical modelling of the transient radon diffusion through radon-proof membranes, can be used as powerful tools for the determination of the radon diffusion coefficient from the measured data sets. The great advantage of the applied mathematical solution is that it enables the determination of the radon diffusion coefficient from any data set obtained by all known measuring modes used throughout Europe. This is very helpful – especially in the present situation where no uniform measuring method exists within Europe.

The numerical modelling of the time-dependent radon diffusion through radon-proof membranes can be also used for the clarification of possible effects that can influence the accuracy of any measurement method. The minimal radon concentration in the source container and the time required for the establishment of steady-state conditions are among the most important parameters, which can be predicted by such a numerical simulation. The most outstanding output from the modelling is the assessment of the time-dependent radon concentration profile within the measured radon-proof membrane, because the shape of the radon distribution curve has a strong influence on the choice of the mathematical model for the calculation of the radon exhalation rate from the membrane.

Acknowledgement

This paper has been supported by the Research Project MSM 6840770005.

References

[1] Spoel WH. Radon transport in sand. Laboratory Study. Technische Universiteit Eindhoven; 1998.
[2] Wójcik M, Wlazlo W, Zuzel G, Heusser G. Radon diffusion through polymer membranes used in the solar neutrino experiment Borexino. Nuclear Instruments and Methods in Physics Research – Section A 2000;449(1–2):158–71.
[3] Löfström R. Report P301547 A. Boras: SP Swedish National Testing and Research Institute; 2003.
[4] Jiránek M, Fronka A. New technique for the determination of radon diffusion coefficient in radon-proof membranes. Radiation Protection Dosimetry 2008;130(1):22–5.
[5] Fernández PL, Quindós LS, Sainz C, Gómez J. A theoretical approach to the measurement of radon diffusion and adsorption coefficients in radonproof membranes. Nuclear Instruments and Methods in Physics Research – Section B 2004;217(1):167–76.
[6] Jiránek M, Hulka J. Radon diffusion coefficient in radon-proof membranes – determination and applicability for the design of radon barriers. International Journal on Architectural Science 2000;1(4):149–55.
[7] Jiránek M, Svoboda Z. Numerical modelling as a tool for optimisation of subslab depressurisation systems design. Building and Environment 2007;42(5):1994–2003.
[8] Zienkiewicz OC, Taylor RL. The finite element method. 5th ed. Oxford: Butterworth-Heinemann; 2000.
[9] Svoboda Z. Software packages TransRn & IterRn, version 2008. Prague: Czech Technical University; 2008.